International Research Journal of Engineering and Technology (IRJET) e-ISSN: 2395-0056
Volume: 04 Special Issue: 09 | Sep -2017 www.irjet.net p-ISSN: 2395-0072
One Day International Seminar on Materials Science & Technology (ISMST 2017)
4th August 2017
Organized by
Department of Physics, Mother Teresa Women's University, Kodaikanal, Tamilnadu, India

Study on optical, magnetic and structural Properties of $NiCoFe_2O_4$ by Co-precipitation technique

D. Anceila[1], G. Francisco Nirmala[1], P. Sagayaraj[2] and V.Joseph[2*]

[1] Department of Physics, Stella Maris College, Chennai-600 086, India
[2,]Department of Physics, Loyola College, Chennai-600 034, India*

Abstract - *Spinel structured nano materials have been extensively studied for the past few decades owing to its excellent biological applications and also its viability in advanced technological areas. Among the class of ferrites, Nickel cobalt ferrite is considered as an interesting candidate for super capacitor applications. It is reported that the structural and magnetic properties may vary with synthesized techniques, therefore it would be very interesting to investigate the structural and magnetic properties of Nickel cobalt ferrite nanoparticles synthesized by varying the pH from 9 and 12 by co-precipitation method. Synthesized samples were characterized by powder X-ray diffraction and found that the sharp diffraction peaks are attributed to its significant crystalline nature of the synthesized products. The crystallite sizes were estimated to be around 9 and 14 nm for the samples synthesized with pH 9 and 12. This shows that as the pH increases, the crystallite size increases, corresponding to the prominent plane (311). UV-Visible spectral analysis (UV) reveals the optical properties and gives spectral information, the optical band bap was found to be 1.93 eV using Kubelka- Munk plot. The FT-IR measurements were carried out in the frequency range of 4000-400 cm^{-1}. TEM investigations revealed the size and shape of nanoparticles. Using vibrating sample magnetometer, the magnetic behaviour of the materials have been determined as a function of magnetic field at room temperature; the magnetic measurements demonstrated that the magnetic behaviour changed from weak ferromagnetic to super paramagnetic as the crystallite size decreases.*

Key Words: $NiCoFe_2O_4$;Co-precipitation; Super paramagnetic.

1.INTRODUCTION

Ferrites engage in recreation of feasible device applications, owing to their structure, enthrallingly active magnetic and electrical properties. When spanned to electrical industries, their steep electrical resistivity is exploited for preventing induction of eddy currents and the resultant loss of energy. Ferrites are thriftily viable and their magnetic and mechanical properties can be customized as per the requirement for device fabrication. As an efficient member of ferrite family, $NiCoFe_2O_4$ has attracted researchers because of its invigorating magnetic properties than other spinel ferrites. The bulk $NiCoFe_2O_4$ belongs to normal spinel type with antiferromagnetic properties below the Néel temperature peaked at 10.5 K whereas it behaves as a paramagnetic candidate at room temperature. All the Ni^{2+} ions reside in the tetrahedral sites (A sites) and the Fe^{3+} ions are totally in the octahedral sites (B sites). In 1961, Néel suggested that the presence of traces of antiferromagnetic particles can exhibit superparamagnetism and weak ferromagnetism due to uncompensated spins in the two sub-lattices. It is worth mentioning that the device design magnetic parameters, namely coactivity, saturation magnetization, magnetic resonance and loss depend on the particle size of Nickel Cobalt ferrite nanoparticles. On the unswerving application side, $NiCoFe_2O_4$ function as MNPs have potential applications in different fields, such as diagnosis of diseases, magnetic resonance imaging, sensors, actuators, magnetic storage devices, biomedical applications etc. The synthesis techniques have a deliverable shaping index or impact in tuning the physical and chemical properties and device fabrication. The properties of synthesized materials can be controlled by understanding crystal structure, the presence of pores, specific surface area and density. The dispensation ways to synthesize $NiCoFe_2O_4$ nanoparticles are many such as micro-emulsion technique , co-precipitation route , ball milling, sol-gel channel, hydrothermal method, ceramic process, and ultrasonic cavitation-assisted solvo thermal synthesis. Among these, co-precipitation is an unsophisticated technique to prepare spinel structured ferrite nanoparticles at low temperatures as it offers the reward in excess than other techniques such as controlled crystallite size, high limpidness, no agglomeration of the particles and latent to amend the particle surface along with homogeneity.

2. Material Synthesis

Analytically graded Merck reagents Nickel chloride ($NiCl_2$), Cobalt chloride ($CoCl_2$) and ferric chloride ($FeCl_3$) was used as such without further purification. Initially, $NiCl_2$ and $CoCl_2$ (0.1 M) and $FeCl_3$ (0.2 M) were dissolved in 75 mL of distilled water separately and stirred well to attain homogenisation. Then NaOH of 2 M solution was used as the mineralizer, which was added drop-wise into the $FeCl_3$ solution under continuous stirring in order to get pH value adjusted to 9. Finally, $NiCl_2$ and $CoCl_2$ solutions was added to the above admixed solution and the temperature was raised to 80 °C for 3 hours until brown precipitate is obtained. The precipitate was centrifuged, thrice with double distilled water and ethanol. The byproduct thus obtained was dried at 75 °C for 24 hours in a hot air oven and was then followed by calcination at 500 °C for 5 hours to obtain the final required product of $NiCoFe_2O_4$ nanoparticles. The experiment was repeated several times by raising the pH to 12 until consistency was achieved.

3.Results and discussion

Crystalline nature and phase formation of the $NiCoFe_2O_4$ powder were identified by recording their X-ray diffractograms using Bruker AXS D8 Advance instrument with CuKα radiation (λ=1.540598 Å) in the 2θ range 20 - 70°. The XRD profile of the synthesized nanomaterials is shown in Fig.1 diffraction peaks and their relative intensities matches very well with the JCPDS card no.22-1024. Hence the observed patterns have been clearly endorsed to the presence of spinel structure. The particle size of the co-precipitated products strongly depends on pH of the precipitation medium and molarity of the precursor. At higher pH values, the decrease in molarity of the solution causes the reduction in particle size. The most prominent peak corresponding to (311) plane is used to calculate approximate size of the particle by using Scherrer equation,

$$\Phi = \frac{k\lambda}{\beta \cos\theta} \quad (1)$$

The crystallite size of pH 9 and 12 is 8 nm and 14 nm respectively. $NiCoFe_2O_4$ nanoparticles crystallize with the cubic spinel structure having lattice constant with the space group Fd3m (227). Absence of secondary phases of CoO, Fe_2O_3 confirmed the formation of phase pure Nickel ferrite nanoparticles. The lattice constant, X-ray density and the porosity was calculated by the below relations,

$$a = d(h^2 + k^2 + l^2)^{\frac{1}{2}} \quad (2)$$

$$d_x = \frac{8M}{Na^3} \quad (3)$$

$$P = 1 - \frac{d}{d_x} \quad (4)$$

Where, in Eq. (2) *a* is the lattice constant, (*h k l*) are the Miller indices and *d* is the inter-planar spacing, in Eq.(3) M, *N,* and *a* represents molecular weight, Avogadro number and lattice constant of $NiCoFe_2O_4$, in Eq. (4) *d* is the bulk density, whereas d_x is the X-ray density structural parameters are been calculated and summarized in Table.1. As the size of nanoparticles reduces, surface effects could become more significant due to the increased volume fraction of surface atoms. Fourier transform infrared spectroscopy analysis carried out on a Perkin Elmer spectrometer using KBr pellet technique in the range of 4000 - 400 cm^{-1}. FTIR imparts information about the presence of functional groups and nature of molecular bonds in the synthesized products. Fig. 2 illustrates the FTIR spectra of Nickel ferrite nanoparticles synthesized with pH 9 and 12. The spectra were recorded in the wave number region from 4000 cm^{-1} to 400 cm^{-1} at room temperature. The high frequency bands are very sensitive to the changes in the interaction between oxygen and cation in octahedral and tetrahedral positions. The main characteristic absorption bands of $NiCoFe_2O_4$ occur at 417 cm^{-1}, 463 cm^{-1}, 544 cm^{-1} and 547 cm^{-1} correspond to metal-oxygen stretching vibrations located at tetrahedral and octahedral positions. The strong absorption peaks at 1615 and 1634 cm^{-1} are attributed to the adsorbed stretching mode of water due to moisture. The absorption peaks at 1615 and 1634 cm^{-1}, 3430 and 3449 cm^{-1} are corresponding to stretching vibrations O-H groups which confirms the presence of water in the sample. The considerable shifts of band observed in the spectra are the cause of the decrease in particle size by increasing pH of the solution. The optical reflectance spectra were recorded on a Varian in the wavelength range of 300 – 800 nm. Ultraviolet-visible spectroscopy (UV-Vis or UV/Vis) refers to absorption spectroscopy or reflectance spectroscopy in the ultraviolet-visible spectral region (i.e. 350 – 1100 nm) of the electromagnetic spectrum. UV–vis spectra in Fig. 3 for $NiCoFe_2O_4$ sample are recorded in the range 600–700 nm. All spectra exhibit a broad absorption region covering 600–700 nm. The two eruditions could be derived from the spectra, the band gap energy and the presence of

spinel defects. For the analysis, the band gap energy was estimated using tauc plot; the optical absorption coefficient near band edge is given by the equation,

$\alpha hv = A(hv - Eg)^{1/2}$ (5) The estimated bandgap was found to be 1.9 and 2.1 eV respectively, as the pH increases the bandgap decreases shown in Fig. 4. In pH 12 there is a slight red shift when compared to bulk $NiCoFe_2O_4$ NP's bandgap. The particle size and morphology of the powder was investigated by Transmission Electron microscope (TEM) model Joel/JEM 2100. The random orientation of particles allows for a statistical measure of the size distribution to be generated. Fig. 5 and 6 reflects the typical TEM micrograph of the $NiCoFe_2O_4$ sample prepared by co precipitation method. The pH had no obvious influence on the morphology, but it affects the crystalline size which demonstrates that the $NiCoFe_2O_4$ nanoparticles were mono disperse and cubically spherical shape with average distributed grain size of pH 9 and 12 was found to be ~ 8 nm and ~ 13 nm, which is smaller than Scherrer calculation. The magnetic properties of fine particles were examined using a vibrating sample magnetometer (VSM) Lakeshore VSM 7407 with magnetic field 2.5 T at room temperature. In Fig. 7 the hysteresis loops are found to be extremely narrow in pH 9; for the reason that the assembly of nanoparticles are with small average diameter. The square ness ratio for the particles is also extremely small. This aspect reflects the nature or gives vital information about the type of domains at hand in the nanoparticles. The corresponding parameters saturation magnetization, retentivity and coercivity values obtained from hysteresis loops are tabulated in Table 2. $NiCoFe_2O_4$ with lower particle size appears to be more superparamagnetic than the larger grain size. This type of behaviour has been attributed to misaligned surface spins due to broken exchange bonds. These spins, fluctuate more freely at high temperatures than those from the core and freeze increasingly at low temperatures into a chaotic structure. As the corecivity increases, the saturation magnetization, retentivity and squareness decreases.

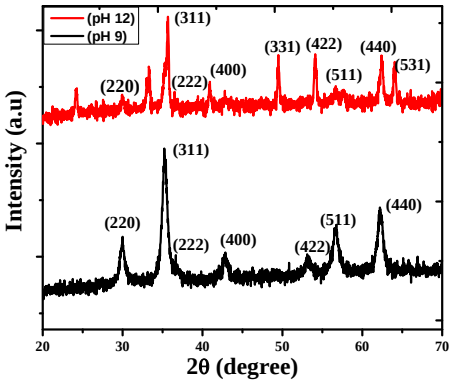

Fig.1 XRD diffraction pattern of $NiCoFe_2O_4$

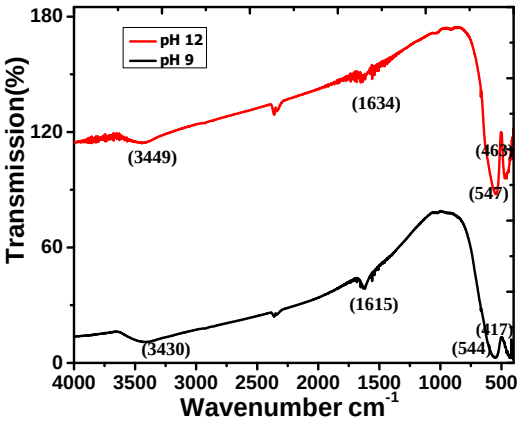

Fig. 2 FTIR spectrum of $NiCoFe_2O_4$ nanoparticles

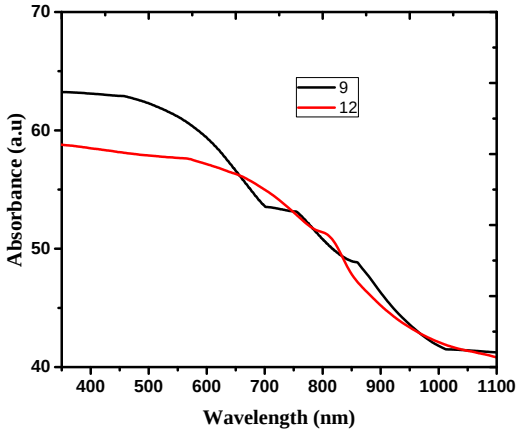

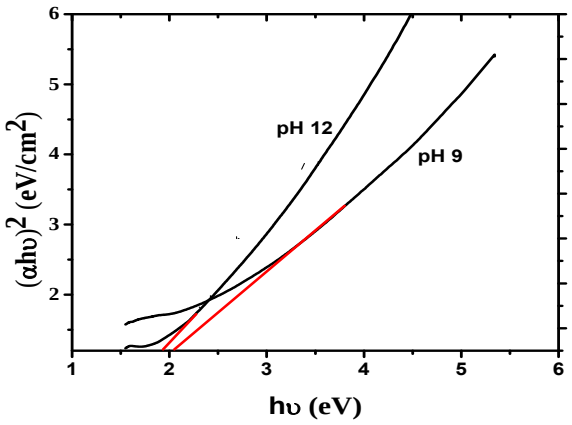

Fig. 3 a) Optical absorption spectra of $NiCoFe_2O_4$nanoparticles as-synthesized using co-precipitation and b) their comparison plot of $(\alpha h\nu)^2$ versus photon energy ($h\nu$).

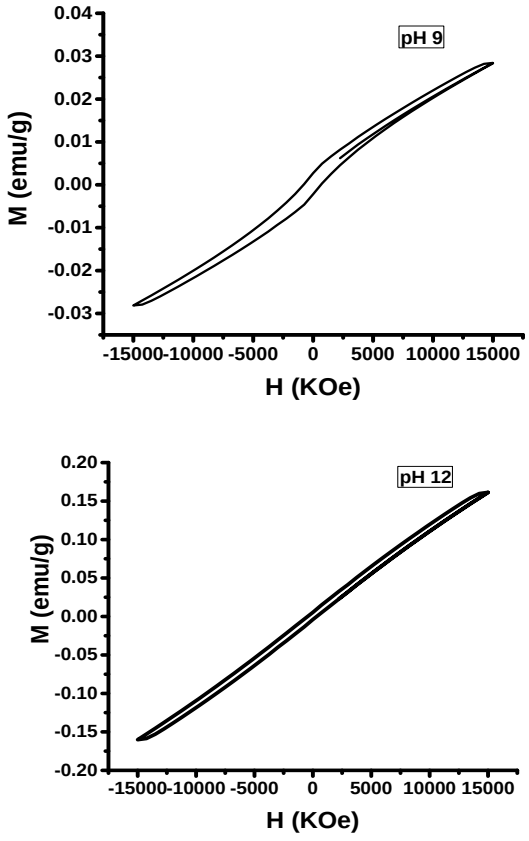

Fig.4 Hystersis loop for $NiCoFe_2O_4$ nanoparticle

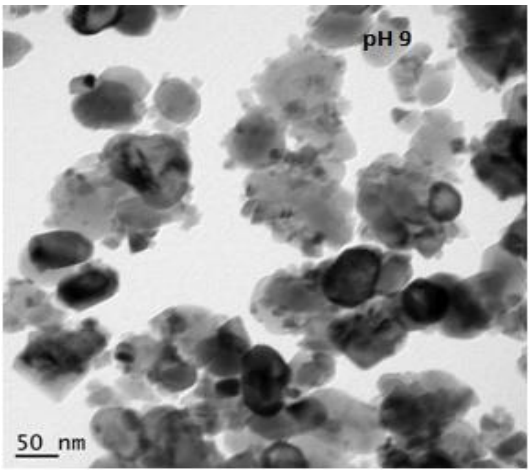

Fig.5 TEM for $NiCoFe_2O_4$ nanoparticle

Table.1. XRD calculations

STRUCTURAL PARAMETERS	pH 12	pH 9
Structure	Spinel cubic	Spinel cubic
Crystallite size (D) (nm)	14	8
Interplaner distance	2.518	2.546
Lattice constant (a)	8.351	8.444
Lattice strain	0.0041	0.0107
Bulk density (d) (gm/cm^3)	4.13	4.13
X-ray density (d_x) (gm/cm^3)	5.498	5.318
Porosity (P) (%)	24.88	22.34

Table.2. VSM

pH	Coercivity Tesla	Sat. Mag. (Ms) emu/gm	Retentivity (Mr) emu/gm	Squareness Mr/Ms
9	394.02	40.07	4.680	0.116
12	578.58	33.77	1.999	0.059

4. Conclusion

In precis, single phase spinel $NiCoFe_2O_4$ nanoparticles were successfully synthesized using co-precipitation method, resulting into small particle size and favourable magnetic properties. It was found that the pH values persuade the reaction mechanism and the crystallite size of the synthesized sample increases with increase in pH value. In FTIR spectrum, the dominant band at 544 and 547 cm^{-1} correspond to metal-oxygen stretching vibrations located at tetrahedral and octahedral positions.

The TEM image of $NiCoFe_2O_4$ nanoparticles gives an idea about the distribution of spherical shape of nanoparticles. VSM measurements publicized weak ferromagnetism with pH value of 12 and at pH value of 9, the ferromagnetic behaviour was concealed and super paramagnetism was observed. We may therefore well conclude that the magnetic properties of $NiCoFe_2O_4$nanoparticles are varied with decrease in crystallite size and considered as a remarkable and potential ternary magnetic material for further investigations and beneficial applications.

REFERENCES

[1] Q. Song and Z.J Zhang, J. Am. Chem. Soc., 134 (2012) 10182-10190.

[2] J. Kennedy, J. Leveneur, G.V. Williams, D.R. Mitchell and A. Markwitz, Nanotechnology, 22 (2011) 115602.

[3] J. Leveneur, J. Kennedy, G.V.M. Williams, J. Metson and A. Markwitz, Appl. Phys. Lett., 98 (2011) 053111.

[4] M.K. Lima-Tenorio, E.A.G. Pineda, N.M. Ahmad, H. Fessi and A. Elaissari, Int. J. Pharm., 493 (2015) 313–327